Carbohydrate Polymers 83 (2011) 569–577

Contents lists available at ScienceDirect

Carbohydrate Polymers

journal homepage: www.elsevier.com/locate/carbpol

Preparation and characterization of carbon nanotube-grafted-chitosan – Natural hydroxyapatite composite for bone tissue engineering

Jayachandran Venkatesan[a], Zhong-Ji Qian[b], BoMi Ryu[a], Nanjundan Ashok Kumar[c], Se-Kwon Kim[a,b,*]

[a] Department of Chemistry, Pukyong National University, Busan 608-737, Republic of Korea
[b] Marine Bioprocess Research Center, Pukyong National University, Busan 608-737, Republic of Korea
[c] Department of Image Science and Engineering, Pukyong National University, Busan 608-739, Republic of Korea

ARTICLE INFO

Article history:
Received 18 June 2010
Received in revised form 10 August 2010
Accepted 11 August 2010
Available online 18 August 2010

Keywords:
Hydroxyapatite
Chitosan
Functionalized multiwalled carbon nanotube
Scaffolds
Bone tissue engineering

ABSTRACT

Porous, biodegradable and biocompatible chitosan, chitosan with natural hydroxyapatite derived from *Thunnus Obesus* bone (chitosan/HAp) and chitosan grafted with functionalized multiwalled carbon nanotube in addition to HAp (*f*-MWCNT-*g*-chitosan/HAp) scaffolds were prepared for the first time via freeze-drying method and physiochemically characterized as bone graft substitutes. The cross-linkages in the novel *f*-MWCNT-*g*-chitosan/HAp scaffold were observed by FT-IR spectroscopy. The water uptake, retention ability and degradation of composite scaffolds decreased whereas thermal stability increased with an addition of HAp and *f*-MWCNT. Uniform dispersion of HAp and *f*-MWCNT in chitosan matrix with interconnected porosity of 70–200 μm (chitosan/HAp) and 46–200 μm (*f*-MWCNT-*g*-chitosan/HAp) was observed by X-ray diffraction, scanning electron microscopy and optical microscopy. Cell proliferation in composite scaffolds was twice than in pure chitosan when checked *in vitro* using MG-63 cell line. These observations suggest that the novel chitosan/HAp and *f*-MWCNT-*g*-chitosan/HAp composite scaffolds are promising biomaterials for bone tissue engineering.

1. Introduction

Over the last four decades, there is a growing interest in the field of artificial organ material preparation, transplantation, surgical reconstruction and the use of artificial prostheses to treat the loss or failure of an organ or tissue. Autograft and allograft are considered ultimate for bone grafting procedure providing osteoconductive and osteoinductive growth factors. However, limitations in donor site, additional surgery, disease transmission and expenditure (Cole et al., 2005; Giannoudis, Dinopoulos, & Tsiridis, 2005) poses a need to develop alternatives to autograft and allograft.

Chitosan, a linear polysaccharide derived from partial deacetylation of chitin, commonly found in shells of marine crustaceans, insects and cell walls of fungi, has been considerably employed in orthopedic applications due to its high biocompatibility, biodegradability, porous structure, suitability for cell ingrowth, osteoconduction and intrinsic antibacterial nature (Di Martino, Sittinger, & Risbud, 2005). The advantage of degradable polymeric implants eliminates the need for a second operation and accelerates new bone growth (Hu, Li, Wang, & Shen, 2004). Low interconnected porosity for cell attachment and mechanical strength of chitosan-based composite biomaterials needs to be improved. However, single component system cannot assist and mimic all the properties of bone and hence developing multicomponent system as an alternative for bone repair becomes mandatory.

Calcium phosphate mineral, hydroxyapatite [$Ca_{10}(PO_4)_6(OH)_2$] (HAp) is considered to play a vital role in various fields including spinal fusion, craniomaxillofacial reconstruction, bone defects, fracture treatment, total joint replacement (bone augmentation) and revision surgery (Best, Porter, Thian, & Huang, 2008; Palmer, Newcomb, Kaltz, Spoerke, & Stupp, 2008). Several authors reported that carbonated HAp has higher osteoconduction, bioresorption and biocompatibility (Landi, Celotti, Logroscino, & Tampieri, 2003; Orr, Villars, Mitchell, Hsu, & Spector, 2001) as compared to synthetic HAp. When compared to natural HAp, the composite of chitosan with synthetic HAp is more widely used as a bone graft substitute (Thein-Han & Misra, 2009). Natural HAp derived from pig bone combined with chitosan has been investigated by some researchers for bone regeneration (Tang et al., 2008; Yuan, Chen, Lü, & Zheng, 2008), no marine source of HAp has been explored so far.

* Corresponding author at: Department of Chemistry, Pukyong National University, Busan 608-737, Republic of Korea. Tel.: +82 51 629 7097; fax: +82 51 628 8147.
E-mail address: sknkim@pknu.ac.kr (S.-K. Kim).

0144-8617/$ – see front matter © 2010 Elsevier Ltd. All rights reserved.
doi:10.1016/j.carbpol.2010.08.019

Recently some tricomponent systems have also been developed with improved cell proliferation on the composite scaffolds as compared to chitosan scaffold. Several authors have addressed the use of tricomponent system for bone tissue engineering including poly(methyl methacrylate) (Kim et al., 2004), gelatin (Li, Chen, Yin, Yao, & Yao, 2007), collagen (Zhang, Tang, Zhang, Xu, & Wang, 2010), poly (L-lactide acid) (Niu, Feng, Wang, Guo, & Zheng, 2009), polycaprolactone (Xiao, Liu, Huang, & Ding, 2009), carboxymethyl cellulose (Jiang, Li, & Xiong, 2009), polyamide 66 (Mu et al., 2006) and montmorillonite (Katti, Katti, & Dash, 2008) with chitosan/HAp.

Despite high mechanical properties for bone tissue growth, collagen formation and biocompatibility (Nien & Huang, 2010), to the best of our knowledge, there are no reports on chitosan grafted with CNT in additon to natural HAp for improved biocompatibility and cell growth for bone tissue engineering which may be because of cytotoxicity issues (Spear & Cameron, 2008). This study aims at incorporating carbonated natural HAp (derived from *Thunnus Obesus* bone) and *f*-MWCNT with chitosan matrix, and to use it as a potential approach to enhance the interconnected porosity and thermal stability, increase the cell proliferation and controllable degradation rate.

2. Materials and methods

Chitosan powder (degree of deacetylation 70–90%, with molecular weight 500 kDa) was purchased from Wako Pure Chemical Industries Ltd., Japan. Hydroxyapatite was isolated from *Thunnus Obesus* bone with thermal calcination method (Lee, Choi, Jeon, Byun, & Kim, 1997). Multiwalled carbon nanotube (outer diameter <8 nm, length 10–30 μm) was purchased from cheap tubes.com, USA. Human osteosarcoma (MG-63) cell line was obtained from American Type of Culture Collection (Manassas, VA, USA). Dulbecco's Modified Eagle's Medium (DMEM) was obtained from Gibco BRL, Life Technology (USA). MTT (3-(4,5-dimethyl-2-yl)-2,5-diphenyltetrazolium bromide) was purchased from molecular probes (Eugene, OR, USA). Other reagents used in this experiment were all of analytical grade.

2.1. Isolation of HAp from Thunnus Obesus

The tuna bone was washed with hot water for 2 days to remove the traces of meat and skin. The washed bones were mixed with 1.0% sodium hydroxide and acetone to remove protein, lipids, oils and other organic impurities (bone and sodium hydroxide solid/liquid ratio was 1:50). After thorough washing the bones were ground in a mortar pestle and then dried at 60 °C for 24 h. In thermal calcination method, 2 g of tuna bone was placed in a silica crucible and subjected to a temperature of 900 °C in an electrical muffle furnace for 5 h (Lee et al., 1997).

2.2. Functionalization and purification of carbon nanotubes (CNTs)

Functionalization of the CNTs was carried out the procedure described by An, Nam, Tan, and Hong (2007).

2.3. Preparation of scaffold materials

2.3.1. Chitosan scaffold preparation

1.74 g of high molecular weight chitosan was dissolved in 250 ml of 2% acetic acid solution. The solution was stirred for 6 h on a mechanical stirrer (RW 20.n Labortechik) and sonicated for 1 h to remove the bubbles. This solution was then transferred to appropriate 12 well and 6 well plates with 3 g and 5 g of solution/well, respectively. The samples were further freezed at −80 °C for 5 h and lyophilized with freeze dryer to form scaffolds. The scaffolds were immersed in 10% NaOH solution for 1 day. After 1 day, scaffolds were washed with excess amount of water till the pH became neutral and lyophilized again.

2.3.2. Chitosan/hydroxyapatite (chitosan/HAp) scaffold

1.8 g of high molecular weight chitosan was dissolved in 250 ml of 2% acetic acid solution. The solution was stirred for 6 h and sonicated for 1 h to remove the bubbles. 4.2 g of naturally derived HAp was suspended in 50 ml of water and carefully transferred into the chitosan solution with the help of dropper. The solution was mechanically stirred for 48 h to disperse the HAp particle in the polymer matrix in homogeneous manner. The milky white resultant solution was then transferred to appropriate 12 well and 6 well plates with 3 g and 5 g of solution/well, respectively, and followed by the same procedure as for the chitosan scaffold.

2.3.3. Carbon nanotube-g-chitosan/hydroxyapatite (*f*-MWCNT-g-chitosan/HAp) scaffold

1.74 g of high molecular weight chitosan was dissolved in 220 ml of 2% acetic acid solution. The solution was stirred for 6 h and sonicated for 1 h to remove the bubbles. Simultaneously, *f*-MWCNT was dispersed in water and sonicated for 30 m. The dispersed *f*-MWCNT was slowly added to the stirring chitosan solution and the mixture was stirred for 6 h. At the same time, naturally derived HAp was separately dispersed in minimum amount of water. This HAp-water suspension was added slowly to the chitosan/*f*-MWCNT mixture and mechanically stirred for 48 h. Finally, this black colored mixture was transferred to appropriate 12 well and 6 well plates with 3 g and 5 g of solution/well, respectively and followed by the same procedure as for the chitosan scaffold.

2.4. General characterization

2.4.1. Porosity measurement

The total porosity was determined by the liquid displacement method (Zhang & Zhang, 2001). The procedure was as follows: first, the volume and weight of the scaffolds were measured, noted as V_0 and W_0, respectively. Secondly, the sample was immersed into the dehydrated alcohol for 48 h until it was saturated by absorbing dehydrated alcohol, and the sample was weighed again and noted as W_1.

Finally, the porosity of the sample was calculated based on the following formula

$$P = \frac{W_1 - W_0}{\rho V_0}$$

where 'ρ' represents the density of dehydrated alcohol, three parallel sets were analyzed for every scaffold and the mean value of the porosities of different scaffolds was achieved.

2.4.2. Water uptake and retention abilities

The water uptake and retention ability of scaffold was studied using the following procedure. Dry scaffolds were weighed (W_{dry}) and immersed in distilled water for 24 h. Then the scaffolds were gently removed from the beaker after 24 h and placed on a wire mesh rack. Excessive water was drained and scaffolds were weighed (W_{wet}) after 5 m to determine water uptake. To measure the water retention ability, the wet scaffolds were transferred to centrifuge tubes with filter paper at the bottom, centrifuged (Combi 514-Hanil Science Industrial) at 500 rpm for 3 m and weighed immediately (W'_{wet}). The percentage of water absorption (E_A) and water retention (E_R) of the scaffolds at equilibrium were calculated using following equation (Hu et al., 2004; Thein-Han & Misra, 2009)

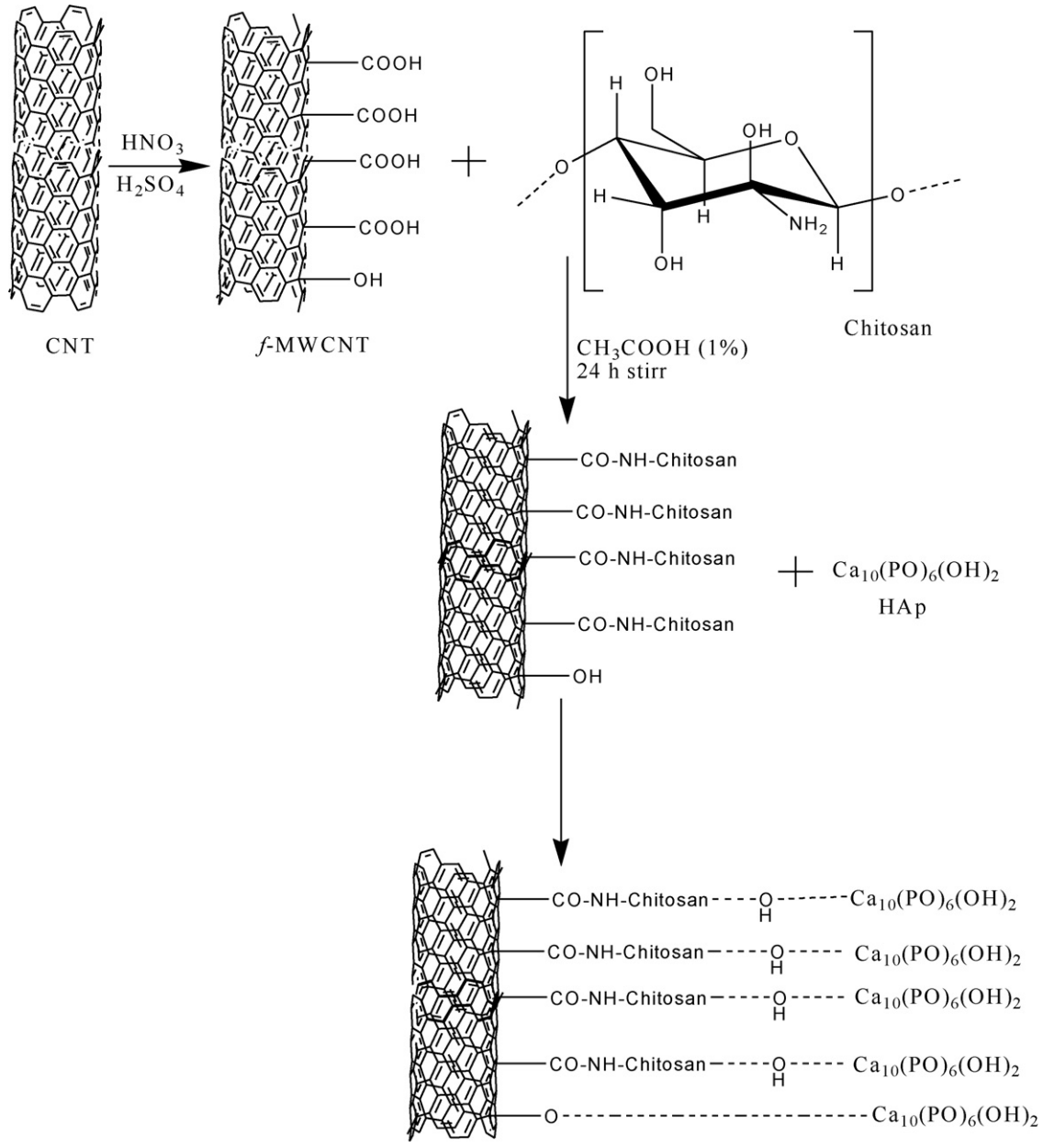

Fig. 1. Scheme of the possible interaction: chitosan, *f*-MWCNT and HAp.

$$E_A = \left[\frac{W_{wet} - W_{dry}}{W_{dry}}\right] \times 100$$

$$E_R = \left[\frac{W'_{wet} - W_{dry}}{W_{dry}}\right] \times 100$$

2.4.3. In vitro degradation with PBS

The degradation of composite scaffolds was investigated by phosphate buffer solution (PBS), 0.1 M PBS has been prepared with sodium phosphate monobasic and sodium phosphate dibasic heptahydrate and pH adjusted 7.2. The samples were immersed in tube containing 10 ml of PBS, kept oscillating at 37.0 ± 0.5 °C. After soaking for 5, 10, 15, 20, 25 and 30 days, the samples was withdrawn, rinsed with deionized water, freeze dried and weighed again. The weight loss (WL) was calculated according to the formula of

$$WL = \frac{W_0 - W_1}{W_0} \times 100\%$$

where W_0 and W_1 denote the weights of sample before and after soaking, respectively. Three parallel samples of the chitosan and their composite scaffolds were used (Jiang et al., 2009)

2.4.4. Thermogravimmetric analysis

Thermogravimmetric analysis was achieved by the use of Pyris 7 TGA analyzer (Perkin-Elmer Inc., USA) with scan range from 50 °C to 900 °C at constant heating rate of 10 °C min^{-1} with continuous nitrogen flow.

2.4.5. FT-IR spectrometry

The stretching frequencies of samples were examined by Fourier Transform Infrared Spectroscopy (Perkin-Elmer, USA) and spectrum GX spectrometer within the range of 600–4000 cm^{-1}.

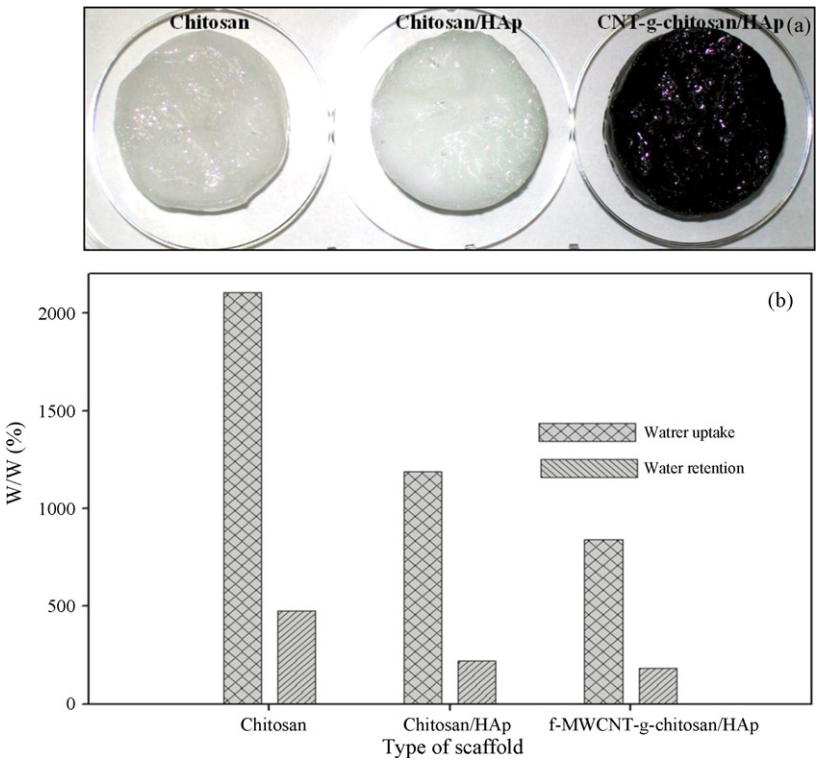

Fig. 2. (b) Water uptakes and water retention ability of chitosan scaffold, chitosan/HAp scaffold and *f*-MWCNT-*g*-chitosan/HAp scaffolds after 24 h. The value is mean standard deviation ($n = 3$).

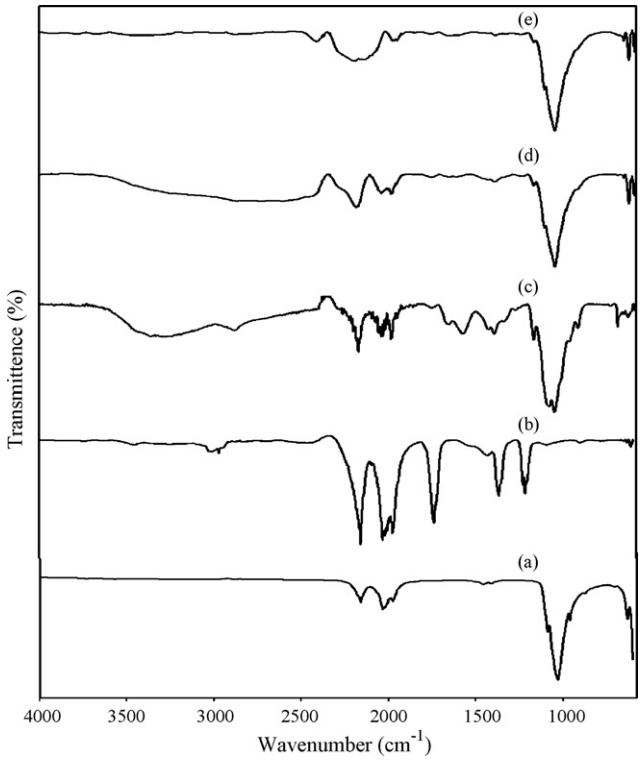

Fig. 3. Infra red spectroscopy images of (a) hydroxyapatite (b) functionalized multiwalled carbon nanotube (c) chitosan scaffold, (d) chitosan/HAp scaffold, (e) *f*-MWCNT-*g*-chitosan/HAp scaffold.

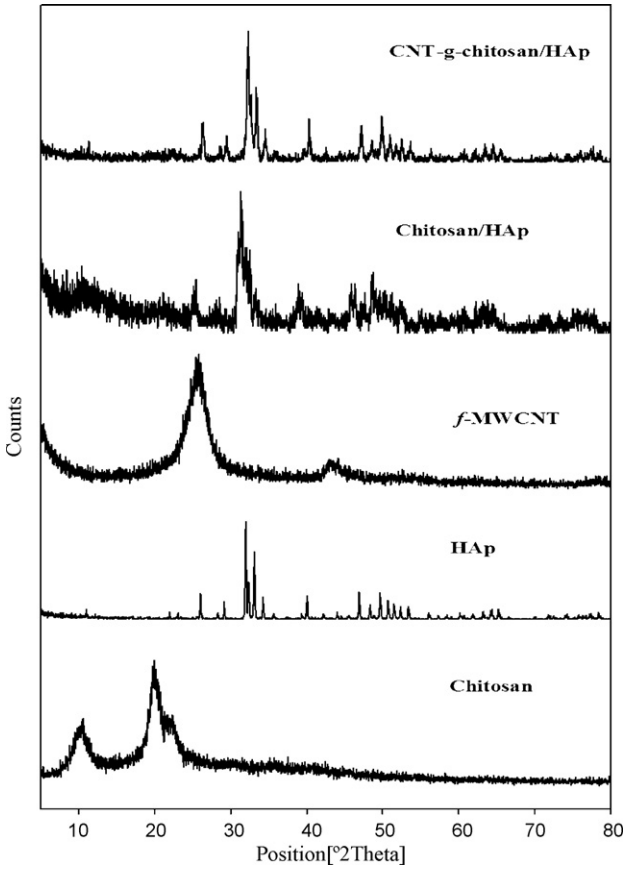

Fig. 4. XRD spectrums of chitosan, HAp, *f*-MWCNT, chitosan/HAp scaffold, *f*-MWCNT-*g*-chitosan/HAp scaffold.

2.4.6. X-ray diffraction analysis

The phase and crystallinity were evaluated using X-ray diffractometer (PHILIPS X'Pert-MPD diffractometer, Netherland) and Cu

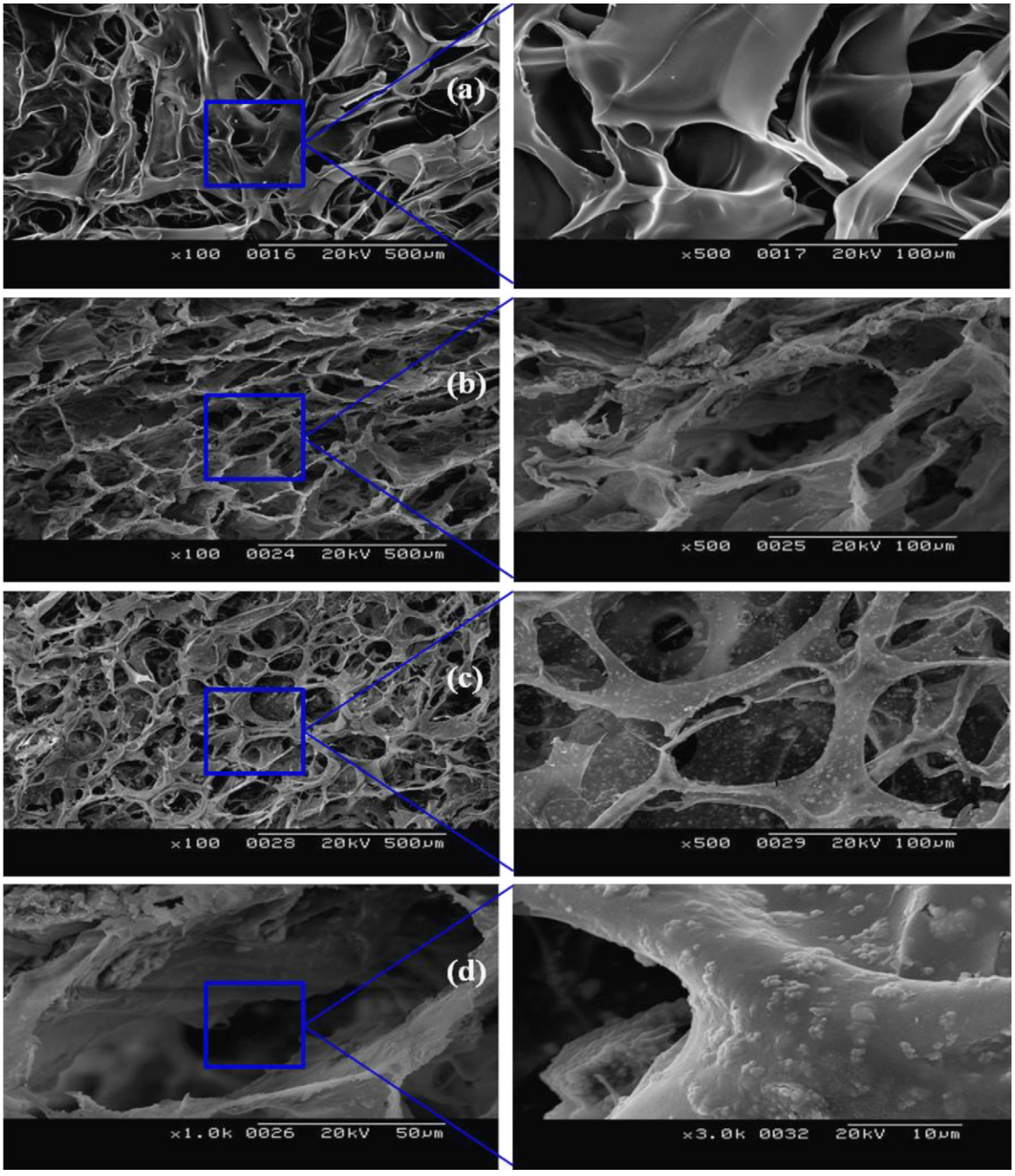

Fig. 5. SEM images of (a) chitosan scaffold (b) chitosan/HAp scaffold (c) *f*-MWCNT-*g*-chitosan/HAp scaffold and (d) dispersion of HAp particles in chitosan matrix.

Kα radiation (1.5405 Å) over a range of 5–80° angle, step size 0.02, scan speed 4°/min at 40 kV and 30 mA.

2.4.7. Scanning electron microscopy and optical microscopy analysis

Porosity and morphology of scaffolds were studied by scanning electron microscopy (SEM HITACHI S-2400, Japan). Optical image of the scaffolds were obtained using optical microscope (Leica, Leica Microsystems Ltd. made in Germany).

2.4.8. In vitro cytotoxicity assay

MG-63 cells (human osteosarcoma cell line) were cultured in DMEM medium supplemented with 5% fetal bovine serum, 2 mM glutamine and 100 μg/ml penicillin–streptomycin and incubated at 37 °C, humidified atmosphere with 5% CO_2. The *in vitro* effects of scaffolds on MG-63 cytotoxicity and cell proliferation were determined by measuring MTT dye absorbance by living cells.

The cells were grown at a concentration of 3×10^5 cells/wells in 6 well plates. After 24 h, cells were washed with fresh medium and were treated with two different concentrations (10 and 20 mg ml^{-1}) of scaffold materials. The cells without the addition of scaffold material were taken as control. After 48 h incubation, cells were rewashed and 100 μl of MTT (1 mg ml^{-1}) was added and further incubated for 4 h. Finally dimethyl sulfoxide was added to solubilize the formazan salt formed and the amount of formazan salt was determined by measuring the OD at 540 nm using aGENios® microplate reader (Tecan Austria GmbH, Austria). The

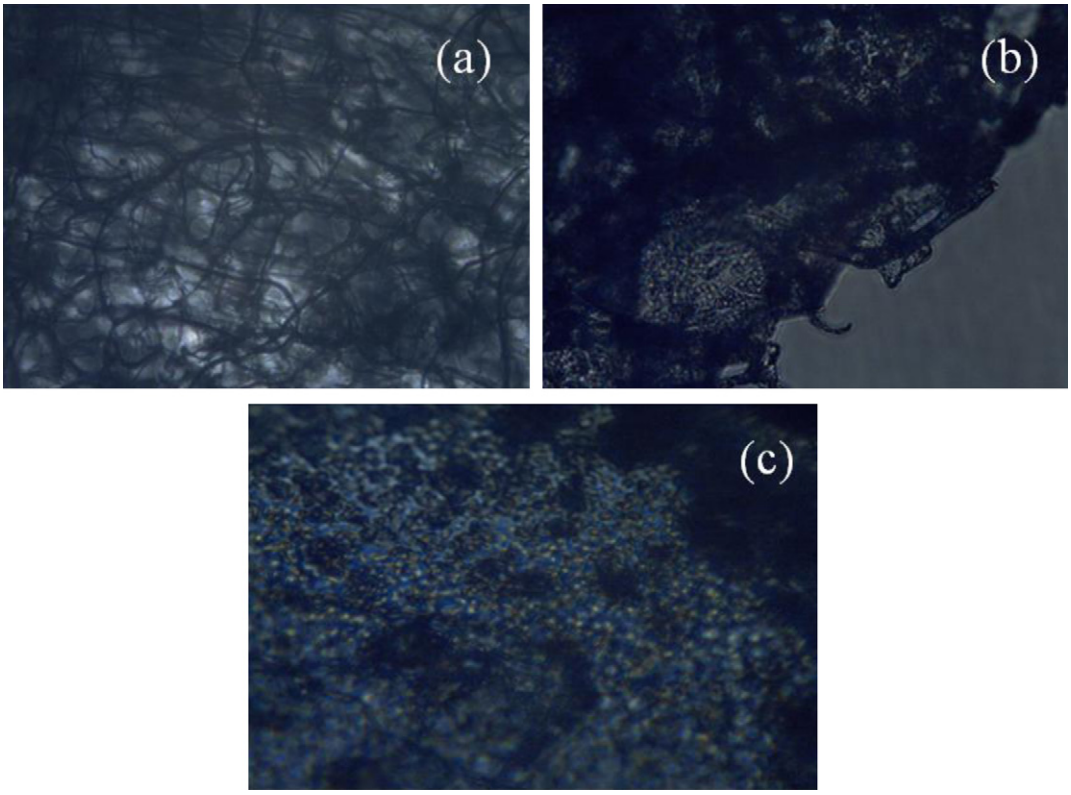

Fig. 6. Optical microscopy images of (a) chitosan scaffold, (b) chitosan/HAp scaffold, (c) *f*-MWCNT-*g*-chitosan/HAp scaffold.

relative cell viability was determined by the amount of MTT converted into formazan salt. Viability of cells was quantified as a percentage compared to that of control.

For cell proliferation on the scaffolds, three replicates of each scaffold were placed into 24 well cell culture plates, and 3.7×10^4 cells/well cell suspension were seeded drop wise on the scaffolds. Then the scaffolds were incubated at 37 °C for 4 h to allow the cells to attach on the materials, 1.5 ml of fresh media was subsequently added in each well. Cell culture without the sample was taken as control. After 1, 2 and 3 days of culture, media was removed and cytotoxicity assay was performed via MTT assay.

3. Results and discussion

3.1. Material selection and scaffold preparation

In this study, we have used three raw materials like chitosan, HAp, *f*-MWCNT which can mimic the all qualities of extracellular matrix of bone such as biocompatibility, biodegradability, and bioactivity. HAp was used as the major component of the scaffolds which was obtained from the by-products of processed *Thunnus Obesus* (Tuna) bone. It was chosen, as the processed wastes of tuna bone increases selectivity to isolate carbonated HAp and also decreases the environmental pollution. As already mentioned carbonated HAp has higher osteoconduction, bioresorption and biocompatibility (Landi et al., 2003; Orr et al., 2001). CNT was used to increase the mechanical strength but pristine CNT is reported to be toxic to cells, therefore functionalization of CNT is important for reduction of toxicity (Abarrategi et al., 2008). Addition of COOH, dispersion increases in the aqueous phase thereby making it suitable for scaffold preparation by possible interactions with other cationic molecules.

To mimic the properties of natural bone, 70% of HAp, 29.9–30% of chitosan and 0.1% of *f*-MWCNT was used as content in the scaffolds. In the basis for the selection of this percentage was the fact that natural bone contains 70% HAp and ~30% of collagen which is a connective protein. Therefore the scaffolds prepared in this study may be more efficient than those previously described. The basis to choose chitosan as the extracellular matrix is its high affinity for HAp and the hydrophilic character which facilitates homogeneous distribution of an aqueous solution containing HAp and *f*-MWCNT. The hydrophilic nature of chitosan and HAp also facilitates cell adhesion, proliferation and differentiation (Thein-Han & Misra, 2009).

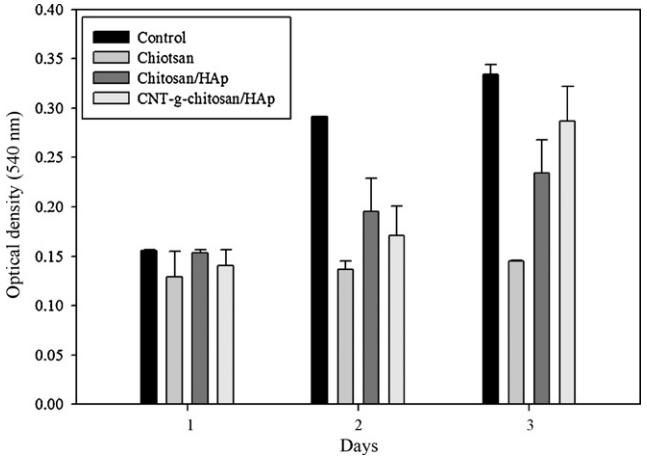

Fig. 7. Cell proliferation of MG-63 cells on scaffold as a function of time, measured by MTT assay which represents active mitochondrial activity of living cells. Optical density was significantly higher on the composite scaffold on day 3 compare to pure chitosan scaffold.

3.2. Gross examination of the scaffolds

The visual examination of lyophilized raw chitosan and their composite scaffolds showed that they are stiff and inelastic. It was observed that the chitosan scaffold swelled rapidly and was more flexible as compared to chitosan/HAp and *f*-MWCNT-*g*-chitosan/HAp scaffolds whereas the composite scaffolds were found to be more rigid. This property is assumed to be due to incorporated HAp and *f*-MWCNT. The chemical basis may be the intermolecular hydrogen bonding interaction between the carboxylic groups present in the *f*-MWCNT's and the NH_2 group of chitosan and OH group of HAp, as shown in Fig. 1. Chitosan and chitosan/HAp scaffolds were obtained in colorless state whereas *f*-MWCNT-*g*-chitosan/HAp was deeply black in color; it may be due to dispersion of the *f*-MWCNT in the polymer and ceramic matrix. Furthermore, all the scaffold materials were found to be very stable in water, they retained their original morphologic arrangement and no degradation was observed initially.

3.3. Porosity measurement

The total porosity of the scaffold was estimated using liquid displacement method; porosity of chitosan scaffold was higher (92.9%) as compared to chitosan/HAp (90.2%) and *f*-MWCNT-*g*-chitosan/HAp (86.74%) scaffolds. In chitosan/HAp scaffold, some chemical interaction may occur between the NH_2 group of chitosan and OH group of HAp which decreases the porosity. Similar reason may be assigned to the further reduced total porosity of the *f*-MWCNT-*g*-chitosan/HAp scaffold; this might be due to interaction between NH_2 groups of chitosan, COOH group of *f*-MWCNT and some additional coordination interactions with the calcium ions of HAp.

3.4. Water uptake and retention abilities

The prepared scaffolds have been shown in Fig. 2a. Since the synthesized chitosan, chitosan/HAp and *f*-MWCNT-*g*-chitosan/HAp composite scaffolds were aimed for bone tissue engineering. The water uptake and water retention ability of chitosan scaffold was higher when compared to chitosan/HAp and *f*-MWCNT-*g*-chitosan/HAp scaffolds (Fig. 2b). As evident from the results, addition of HAp and *f*-MWCNT to pure chitosan leads to a decrease in the degree of water absorption. Furthermore, the water retention ability of chitosan/HAp and *f*-MWCNT-*g*-chitosan/HAp scaffolds were comparable with slight difference but were much less when compared to the pure chitosan scaffold. This might be partially due to the addition of ceramic and hydrophobic character of *f*-MWCNT. Similar trends of decreases in water absorption with increases in the content of HAp have been previously reported (Thein-Han & Misra, 2009). Since HAp is a prominent component of natural bone and we have used similar percentage of HAp (70%) for scaffold preparations, the low values of water retention by the chitosan/HAp and *f*-MWCNT-*g*-chitosan/HAp scaffolds can be justified and these scaffolds can still be used for bone tissue engineering.

3.5. In vitro degradation with PBS

Chitosan has been shown to be degraded by PBS solution (Jiang et al., 2009), which mimics the exact intracellular environment in human body fluids and tissues. In this study, we have chosen 0.1 M PBS as soaking solution; a suitable and reliable medium to investigate the degradation and structural stability. The degradation of chitosan, chitosan/HAp and *f*-MWCNT-*g*-chitosan/HAp scaffolds, after soaking in 0.1 M PBS for 30 days, we found that chitosan scaffold was degraded to around 30% of its original weight in 30 days; whereas the degradation rate was slower in chitosan/HAp and *f*-MWCNT-*g*-chitosan/HAp (around 10% degradation in 30 days). The lower degradation of the chitosan/HAp and *f*-MWCNT-*g*-chitosan/HAp scaffold might be due to addition of HAp and *f*-MWCNT into the scaffold materials.

In case of *f*-MWCNT-*g*-chitosan/HAp scaffold, it is assumed that water penetrates into the scaffolds and breaks the linkage between *f*-MWCNT-*g*-chitosan thereby increasing the degradation by producing short polymeric chain from the high polymeric chain. Pompeo and Resasco (2002) proved that amine functionalization of CNT leads to solubilization of CNT in the aqueous media. Solubilization of CNT is an important factor to reduce its toxicity in the cellular environment.

3.6. Thermal stability of the scaffolds

The thermal stability of scaffolds was assessed by TGA analysis. From the TGA and DTG curves, chitosan weight loss was observed at 304 °C which corresponds to chitosan moieties. For composite chitosan/HAp and *f*-MWCNT-*g*-chitosan/HAp scaffolds, weight loss of around 17.8% and 17.12% was observed at 304.12 °C and 302.08 °C, respectively and was attributed to chitosan moieties. The slight temperature difference observed for the *f*-MWCNT-*g*-chitosan/HAp scaffold might be due to some covalent interactions between *f*-MWCNT and chitosan. At temperature as high as 900 °C, chitosan scaffolds lost all the weight whereas no weight loss was observed in the chitosan/HAp and *f*-MWCNT-*g*-chitosan/HAp scaffolds indicative of high thermal stability of HAp. Our results prove that the composite scaffold materials are highly stable at higher temperature.

3.7. Stretching frequency of the scaffolds

In order to illustrate intermolecular interactions between components in the scaffolds, FT-IR spectrum was taken. Fig. 3 shows the FT-IR spectra of HAp, *f*-MWCNT, chitosan, chitosan/HAp and CNT-*g*-chitosan/HAp scaffolds. For HAp, the spectrum showed the characteristic absorption bands of natural HAp reported (Markovic, Fowler, & Tung, 2004). Those bands were $\nu_3(PO_4^{3-})$ stretching at 1031–1089 cm^{-1}, $\nu_1(PO_4^{3-})$ at 962 cm^{-1}, $\nu_4(PO_4^{3-})$ asymmetric bending stretching at 570 cm^{-1}, $\nu_3(CO_3^{2-})$ at 1412–1415 cm^{-1} and $\nu_2(CO_3^{2-})$ at 872 cm^{-1}. For chitosan scaffold, the spectrum showed the typical characteristic absorption bands of chitosan as reported earlier (Thein-Han & Misra, 2009); which are carbonyl group (C=O) at 1736 cm^{-1}, C–H stretching of rock and bending at 1418 cm^{-1} and 1377 cm^{-1}, respectively and amine stretching frequency ν_s(N–H), pyranose ν_3 (C–O–C) stretching mode at 1145 cm^{-1}, 1077 cm^{-1} and 1030 cm^{-1}, respectively. Moreover, the characteristic stretching frequency of *f*-MWCNT was observed at ν(COOH) at 1738 cm^{-1} and OH stretching frequency was observed at 3500 cm^{-1}. CH rock mode of vibration was observed at 1365 cm^{-1}.

FT-IR spectrum of composite chitosan/HAp and *f*-MWCNT-*g*-chitosan/HAp scaffolds contains characteristic peaks of all the raw materials like chitosan, HAp and *f*-MWCNT. FT-IR spectrum of *f*-MWCNT-*g*-chitosan/HAp scaffold depicted a new strong absorbance at 1638 cm^{-1} (corresponding to amide group), indicating that the –COOH groups of *f*-MWCNT reacted with the $-NH_2$ of chitosan and converts it to amide (–CONH–) group. This unique band frequency clearly indicates the formation of graft (*f*-MWCNT-*g*-chitosan) between chitosan and *f*-MWCNT.

3.8. X-ray diffraction studies

The diffraction patterns of chitosan, natural HAp, *f*-MWCNT, chitosan/HAp and CNT-*g*-chitosan/HAp have been shown in Fig. 4. In chitosan scaffold, three main peaks were observed at 10.5°, 20.0° (maximum intensity) and 22.5°, respectively corresponding

to characteristic peaks of chitosan. This peak angle 20.0° was found in all the three scaffolds confirming the presence of chitosan in all the three type of scaffolds. In chitosan/HAp composite scaffold, diffraction peaks was observed at 25.4° and 31.4° which revealed the presence of HAp. In case of *f*-MWCNT-*g*-chitosan/HAp scaffold, strong absorption peaks were observed at 26.3°, 32.3°, 32.7°, 33.4° and 47.1° this indicated the poor crystallinity state of HAp particle in *f*-MWCNT-*g*-chitosan/HAp scaffold.

3.9. Morphology studies of the scaffolds

Fig. 5 shows the SEM images of low and high magnification of (a) chitosan scaffold (b) chitosan/HAp scaffold (c) *f*-MWCNT-*g*-chitosan/HAp scaffold (d) dispersion of HAp in chitosan matrix. The SEM images depicted that the composite scaffolds were three dimensional, with almost equal porous structures and with good interconnectivity. According to the SEM images, HAp particles were uniformly dispersed in the chitosan (Fig. 5d). Interconnected porosity structures are found in the chitosan/HAp and *f*-MWCNT-*g*-chitosan/HAp but absent in the chitosan scaffold. This might be the basis of the flexible behavior of chitosan scaffold. Uniform distribution of HAp particles and *f*-MWCNT in the polymer matrix was observed which may be due to the electrically charged nature of chitosan network.

The pore size of the chitosan/HAp and *f*-MWCNT-*g*-chitosan/HAp scaffold varied from 70 μm to 200 μm and 46 μm to 200 μm, respectively as measured by SEM. Reports suggest that the cell migration and proliferation is higher in scaffolds with large pore size (100 μm) (Thein-Han & Misra, 2009). We can conclude from the pattern of results that the addition of *f*-MWCNT in the polymer and ceramic matrix leads to increases the interconnected pore size.

3.10. Optical microscopy analysis

The dispersion of HAp particles and *f*-MWCNTs in the chitosan matrix was also observed by optical microscopy as shown in Fig. 6. The incident light of optical microscope easily penetrates in the chitosan matrix, whereas HAp and *f*-MWCNT reflect incident light. The optical microscopic image of chitosan clearly indicated improper pore structure whereas; addition of HAp and *f*-MWCNTs polymer matrix improved the porosity. The optical microscopy images of *f*-MWCNT-*g*-chitosan/HAp shows the well-dispersed status of *f*-MWCNTs in the matrix with slight aggregation. This indicated that the *f*-MWNTs are uniformly distributed within the chitosan matrix; these results were consistent with the SEM observations.

3.11. In vitro cytotoxicity and cell proliferation

Scaffold for bone tissue engineering necessitates a highly porous and interconnected pore structure to ensure that the biological environment is conductive to cell attachment, proliferation, tissue growth and adequate nutrient flow. The cytotoxicity effects and cell proliferation of respective scaffold were investigated through MTT assay. The cytotoxicity of *f*-MWCNT-*g*-chitosan/HAp was found no cytotoxicity in MG-63 cell line. The cell viability of scaffold higher then chitosan scaffold. This might due to addition of HAp crystals in the scaffold. Moreover, the entire three scaffolds were found to be non-toxic when tested with MG-63 cell line. The cell proliferation of MG-63 on scaffolds was observed to be twice in the case of composite scaffolds as compared to chitosan scaffold (Fig. 7).

4. Conclusion

We have developed a novel *f*-MWCNT-*g*-chitosan/HAp composite scaffold by freeze-drying method to mimic all the required properties of extracellular matrix of bone. Ions cross-linkage of $[NH_3^+]$ of chitosan with $[COO^-]$ group of *f*-MWCNT and metal interaction of HAp with chitosan in the *f*-MWCNT-*g*-chitosan/HAp scaffold was clearly observed. Based on properties such as good thermal stability, interconnected porosity, controlled *in vitro* degradation and cell proliferation, we conclude that *f*-MWCNT-*g*-chitosan/HAp scaffold is a novel composite scaffold that will have great potential applications in the field of bone tissue engineering.

Acknowledgements

This work was supported by a grant from Marine Bioprocess Research Centre of the Marine Bio 21 Center funded by the Ministry of Land, Transport and Maritime, Republic of Korea.

References

Abarrategi, A., Gutiérrez, M. C., Moreno-Vicente, C., Hortigüela, M. J., Ramos, V., López-Lacomba, J. L., et al. (2008). Multiwall carbon nanotube scaffolds for tissue engineering purposes. *Biomaterials*, *29*(1), 94–102.

An, J. S., Nam, B.-U., Tan, S. H., & Hong, S. C. (2007). Study on thefunctionalization of multi-walled carbon nanotube with monoamine terminated poly(ethylene oxide). *Macromolecular Symposia*, *249–250*(1), 276–282.

Best, S. M., Porter, A. E., Thian, E. S., & Huang, J. (2008). Bioceramics: Past, present and for the future. *Journal of the European Ceramic Society*, *28*(7), 1319–1327.

Cole, D. W, Ginn, T. A., Chen, G. J., Smith, B. P., Curl, W. W., Martin, D. F., et al. (2005). Cost comparison of anterior cruciate ligament reconstruction: Autograft versus allograft. *Arthroscopy: The Journal of Arthroscopic & Related Surgery*, *21*(7), 786–790.

Di Martino, A., Sittinger, M., & Risbud, M. (2005). Chitosan: A versatile biopolymer for orthopaedic tissue-engineering. *Biomaterials*, *26*(30), 5983–5990.

Giannoudis, P., Dinopoulos, H., & Tsiridis, E. (2005). Bone substitutes: An update. *Injury*, *36*(3S), 20–27.

Hu, Q., Li, B., Wang, M., & Shen, J. (2004). Preparation and characterization of biodegradable chitosan/hydroxyapatite nanocomposite rods via in situ hybridization: A potential material as internal fixation of bone fracture. *Biomaterials*, *25*(5), 779–785.

Jiang, L. Y., Li, Y. B., & Xiong, C. D. (2009). A novel composite membrane of chitosan–carboxymethyl cellulose polyelectrolyte complex membrane filled with nano-hydroxyapatite I. Preparation and properties. *Journal of Materials Science: Materials in Medicine*, *20*(8), 1645–1652.

Katti, K., Katti, D., & Dash, R. (2008). Synthesis and characterization of a novel chitosan/montmorillonite/hydroxyapatite nanocomposite for bone tissue engineering. *Biomedical Materials*, *3*(3), 4122.

Kim, S., Kim, Y., Yoon, T., Park, S., Cho, I., Kim, E., et al. (2004). The characteristics of a hydroxyapatite–chitosan–PMMA bone cement. *Biomaterials*, *25*(26), 5715–5723.

Landi, E., Celotti, G., Logroscino, G., & Tampieri, A. (2003). Carbonated hydroxyapatite as bone substitute. *Journal of the European Ceramic Society*, *23*(15), 2931–2937.

Lee, C., Choi, J., Jeon, Y., Byun, H., & Kim, S. (1997). The properties of natural hydroxyapatite isolated from tuna bone. *Journla of Korean Fisheries Society*, *30*, 652–659.

Li, J., Chen, Y., Yin, Y., Yao, F., & Yao, K. (2007). Modulation of nano-hydroxyapatite size via formation on chitosan–gelatin network film in situ. *Biomaterials*, *28*(5), 781–790.

Markovic, M., Fowler, B., & Tung, M. (2004). Preparation and comprehensive characterization of a calcium hydroxyapatite reference material. *Journal of Research of the National Institute of Standards and Technology*, *109*(6), 553–568.

Mu, Y., Li, Y., Xiang, H., Zhang, X., Zhang, L., Wu, L., et al. (2006). The preparation and characterization of porous scaffold made of nano-hydroxyapatite/chitosan/polyamide 66 composite. *Gaofenzi Cailiao Kexue yu Gongcheng*, *22*(5), 213–216.

Nien, Y.-H., & Huang, C.-l. (2010). The mechanical study of acrylic bone cement reinforced with carbon nanotube. *Materials Science and Engineering B*, *169*(1–3), 134–137.

Niu, X., Feng, Q., Wang, M., Guo, X., & Zheng, Q. (2009). Porous nano-HA/collagen/PLLA scaffold containing chitosan microspheres for controlled delivery of synthetic peptide derived from BMP-2. *Journal of Controlled Release*, *134*(2), 111–117.

Orr, T. E., Villars, P. A., Mitchell, S. L., Hsu, H. P., & Spector, M. (2001). Compressive properties of cancellous bone defects in a rabbit model treated with particles of natural bone mineral and synthetic hydroxyapatite. *Biomaterials*, *22*(14), 1953–1959.

Palmer, L. C., Newcomb, C. J., Kaltz, S. R., Spoerke, E. D., & Stupp, S. I. (2008). Biomimetic systems for hydroxyapatite mineralization inspired by bone and enamel. *Chemical Reviews*, *108*(11), 4754–4783.

Pompeo, F., & Resasco, D. E. (2002). Water solubilization of single-walled carbon nanotubes by functionalization with glucosamine. *Nano Letters*, *2*(4), 369–373.

Spear, R., & Cameron, R. (2008). Carbon nanotubes for orthopaedic implants. *International Journal of Material Forming*, *1*(2), 127–133.
Tang, X.-J., et al. (2008). Hard tissue compatibility of natural hydroxyapatite/chitosan composite. *Biomedical Materials*, *3*(4), 044115.
Thein-Han, W. W., & Misra, R. D. K. (2009). Biomimetic chitosan–nanohydroxyapatite composite scaffolds for bone tissue engineering. *Acta Biomaterialia*, *5*(4), 1182–1197.
Xiao, X., Liu, R., Huang, Q., & Ding, X. (2009). Preparation and characterization of hydroxyapatite/polycaprolactone–chitosan composites. *Journal of Materials Science: Materials in Medicine*, *20*(12), 2375–2383.
Yuan, H., Chen, N., Lü, X., & Zheng, B. (2008). Experimental study of natural hydroxyapatite/chitosan composite on reconstructing bone defects. *Journal of Nanjing Medical University*, *22*(6), 372–375.
Zhang, L., Tang, P., Zhang, W., Xu, M., & Wang, Y. (2010). Effect of chitosan as a dispersant on collagen-hydroxyapatite composite matrices. *Tissue Engineering Part C Methods*, *16*(1), 71–79.
Zhang, Y., & Zhang, M. (2001). Synthesis and characterization of macroporous chitosan/calcium phosphate composite scaffolds for tissue engineering. *Journal of Biomedical Materials Research*, *55*(3), 304–312.